CARBON 79 (2014) 413–423

Available at www.sciencedirect.com

ScienceDirect

journal homepage: www.elsevier.com/locate/carbon

Enhancement of fracture toughness of carbon fiber laminated composites using multi wall carbon nanotubes

Vahid Mirjalili, Rajaprakash Ramachandramoorthy, Pascal Hubert *

Department of Mechanical Engineering, McGill University, 817 Sherbrooke Street West, Montreal, Québec H3A 0C3, Canada

ARTICLE INFO

Article history:
Received 26 February 2014
Accepted 31 July 2014
Available online 6 August 2014

ABSTRACT

In this paper, the effect of Multi Wall Carbon Nanotubes (MWNT) as a toughening agent of laminated composites is experimentally investigated. Carbon fiber laminates were manufactured by resin film infusion technique in which the resin flows in the through-the-thickness direction. The modified polymer systems showed 17% improvement in the stress intensity factor (K_{Ic}), whereas the laminated composites showed up to 48% improvement in Mode I and 143% improvement in Mode II fracture toughness. Scanning Electron Microscope (SEM) was then used to study the fractured surface and to explain the contrasting behavior of the MWNT-modified polymers when compared to the laminates.

1. Introduction

Composite materials are increasingly used in aerospace, automotive and renewable energy industries. This growth is mainly due to the higher strength-to-weight ratio offered by composites, when compared to metals. A major component of these laminated fiber reinforced composites is a polymer matrix that holds the fibers together. The most widely used polymeric resins are thermoset epoxies that provide high modulus, but low fracture toughness values. Since fibere are mechanically stronger than the matrix, [1], the matrix fracture toughness is the key material property that controls damage initiation and growth in composites, especially in through-the-thickness properties, such as delamination properties. Delamination is one of the major failure mechanisms associated with composites that allow cracks to grow between the plies of a laminate. Most epoxy resins are brittle and have Mode I fracture toughness of about 80–300 J/m^2 in the delamination mode [2–5]. This low fracture toughness value severely limits the full potential of weight reductions offered by composites [6].

There are mainly two solutions to the problem of low fracture toughness in brittle polymers, [7]: (1) using thermoplastic resins instead of thermosetting systems, (2) modifying the brittle thermosetting polymer by adding rubber or inorganic micro-particles. While the former provides a very tough system, the manufacturing process of thermoplastic resins is very expensive. Hence, modifying thermoset resins by adding rubber or inorganic micro-particles becomes a more attractive alternative, mainly because of the easier processing. The rubber toughened epoxies (2–4 kJ/m^2) are tougher than particle filled systems (0.5–1 kJ/m^2), but on the downside elastic properties as well as glass transition temperatures are reduced [7]. These disadvantages open up the opportunity to explore novel nano-particles, such as carbon nanotubes, which have been proved to improve not only elastic and thermal properties of the resin but also the fracture toughness in composites [8,9].

* *Corresponding author.*
E-mail address: pascal.hubert@mcgill.ca (P. Hubert).
http://dx.doi.org/10.1016/j.carbon.2014.07.084
0008-6223/

Several researchers have modelled and experimentally verified the potential of CNTs as a toughening agent in brittle polymer matrixes [10–13], both in Mode I and Mode II delamination resistance mode. These nano-sized particles have shown potential for toughness enhancement at low carbon nanotube (CNT) content, by introducing several toughening mechanisms, such as CNT bridging, crack pinning, and crack deflection, [8]. Another important aspect of adding CNTs to polymers is the enhanced multi-functional properties of the final formulation, such as improved elastic, electrical and thermal properties [14]. However, addition of CNTs to polymers introduces new challenges in the processing of nano-modified polymers, as CNTs increase the viscosity of the base polymer [15], and affect the processing of these nano-modified polymers.

There are two main techniques for the manufacturing of composite laminates modified with CNTs: (1) CNT modification of matrix [12], and (2) CNT modification of fiber [16]. The former has the advantage of being simple and also has a processing method similar to the traditional processing method of composites in the industry. The main difficulties of this technique are due to filtering of CNTs during the impregnation of fiber mat [17,18], and due to the high viscosity of the resin system which leads to major processing issues [15,19–21]. CNT modification of fibers on the other hand has several advantages but has a more complex processing method. This technique resolves the problem of dispersion and aggregation of CNTs during the manufacturing. Also, CNTs are aligned perpendicular to the fibers which is the optimum direction to improve the delamination properties. Whereas for CNT modified resin, direction of the CNTs in the composite tends to be along the flow path [16]. Tugrul Seyhan et al. manufactured their panel using Vacuum Assisted Resin Transfer Molding and observed a decrease in Mode I delamination properties, while the Mode II properties improved by 11% [12]. In this paper, Resin Film Infusion (RFI) technique is used for manufacturing the laminated composites where resin flows in through-the-thickness direction. Hence, it maintains the dispersion quality and provides better alignment of MWNTs in the Z direction.

Another interesting observation with thermoplastic toughening agents as a toughening agent is their synergistic effect when mixed with more traditional toughening agents such as thermoplastic or rubbery particles. A study by Kinloch et al. [22,23] showed a synergistic effect when silica nano particles were combined with rubber toughened epoxy. The silica nano particle which improved the fracture toughness of the base epoxy by 400% became more effective in rubber toughened epoxy (same base epoxy). The nano-modified rubber toughened epoxy was 200% tougher than rubber toughened epoxy and 2200% tougher than the base epoxy. This synergistic effect is studied in the paper by adding a thermoplastic toughening agent to MWNT-modified epoxy.

Other than the unique attribute of the RFI manufacturing technique, and investigation of the synergistic effect, this paper also studies the fracture surface of the test specimen to explain toughening mechanisms that contributed to the 48% and 143% improvement in Mode I and Mode II delamination properties, respectively.

2. Experimental procedure

2.1. Materials

The materials needed for this research was provided by Nanoledge Inc. The base epoxy resin or the neat resin was a hot-melt resin (solid at room temperature), which was a blend of multifunctional epoxy resins. The curing agent, 4,4′-diaminodiphenylsulfone, was used with a hardener-to-resin ratio of 30:100. The MWNTs were commercially bought from Bayer [24]. To apply a hard/soft nano particles synergistic strategy, traditional soft fillers (acrylate based copolymers) were used to get rubbery nano domains in the final composite materials.

Two different formulations were used in this work:

(1) MWNT composites (2377): this formulation contains 0.3 wt.% MWNTs mixed with the hardener and resin (30:100) mixture. The MWNTs were functionalized to develop physical interaction with the matrix with no covalent linkage.
(2) MWNT + thermoplastic toughening agent composites (2378): this formulation was prepared in a similar fashion to the 2377 MWNT composite system except that soft acrylate based thermoplastic toughening agents (4 wt.%) were added to the mixture.

After the preparation of the resin formulation, thin resin films (semi-solid at room temperature) were manufactured using a three roll coater. The areal weight of the resin films were 225 gram per square meter with a thickness of 205 μm. These two resin film formulations were then used to impregnate the carbon fibers manufactured by JB Martin (TC-18-N).

2.2. Specimen preparation

The fracture toughness of the base polymer formulations was first characterized under 3-point bending according to ASTM D 5045-91. For these samples, Single-Edge-Notch Bending (SENB) specimens were prepared according to the ASTM standard. The polymer plates were manufactured by stacking 18 layers of resin films in a closed, pressurized mold. A pressure of 5 bars was first applied at room temperature to the samples. Then using a cure cycle of 2 h hold at 130 °C and 2 h hold at 200 °C with the ramp rate of 3 °C/min the samples were cured. The SENB specimens of 20 mm in length, 4 mm in width and 2.5 mm in thickness were then cut from the cured plates. The pre crack length 'a' was selected such that $0.45 < a/W < 0.55$, following the standard test method outlined in ASTM D5045-91. The first sharp notch was prepared with a depth of 1.7 mm and width of 300 μm using the Accutom model of Struers precision diamond saw. Subsequently, a natural crack was initiated by sliding a fresh razor blade across the notch root with a depth of approximately 300 μm. The SENB samples were tested in a fullam testing stage (shown in Fig. 2) under an optical microscope (Olympus BX-51M) with a 100 lb load cell.

Composite laminates were then manufactured using prepreg and resin film infusion technologies. Test specimens

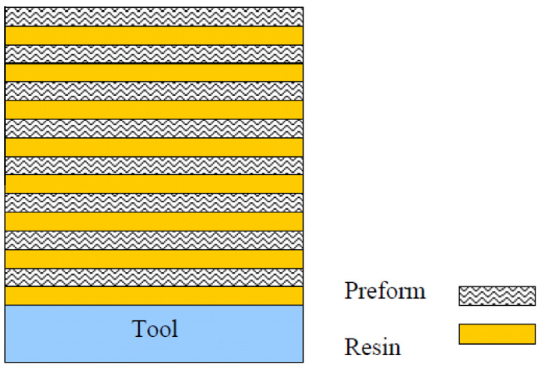

Fig. 1 – Stacking procedure for the MWNT system. (A color version of this figure can be viewed online.)

were cut from the cured laminated. The specimens were tested under pure Mode I (interlaminar tension) and pure Mode II (interlaminar shear) according to the ASTM D5528-01 standard. For each test sample, total of five specimens were tested.

For the interlaminar fracture toughness characterization of MWNT modified composites, Mode I and Mode II fracture tests were carried out using rectangular Double Cantilever Beam (DCB) specimens and rectangular End Notched Flexure (ENF) specimens, respectively. Three panels with each formulation (neat, 2377 and 2378) were manufactured.

Panels of carbon fiber composites were manufactured and specimens with dimensions of $140 \times 20 \times 4.5\ mm^3$ and $170 \times 20 \times 4.5\ mm^3$ (length × width × thickness) were cut from the panel for the Mode I and Mode II testing respectively, according to the ASTM D5528-01 standard [25]. The initial delamination length for the Mode I specimens and Mode II specimens were kept at 50 mm and 30 mm respectively.

2.2.1. *Laminate preparation*

8 layers of fiber preform/resin film were stacked as shown in Fig. 1. This stacking sequence maximizes the infiltration during the curing process and minimizes the MWNT filtration, compared to the Vacuum Assisted Resin Transfer Molding (VARTM) process where MWNTs are filtered during the resin flow.

A 10-micron Teflon film was placed in the mid-plane of the laminates as a crack initiator according to the ASTM standard for Mode I and Mode II; hatched areas in the Fig. 3 represent

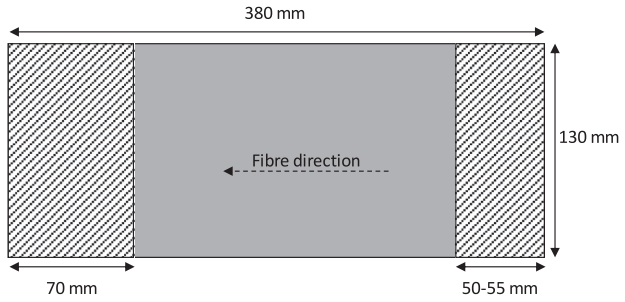

Fig. 3 – Panel size and Teflon insert location.

the Teflon insert. Each panel was vacuum bagged according to the sequence given in Fig. 4 and the samples were cured in an autoclave at 100 psi (applied at the beginning of the cure cycle). The cure cycle was the same as for the SENB polymer samples; 2 h hold at 130 °C and 2 h hold at 200 °C with a ramp rate of 3 °C/min.

2.2.2. *Trimming and cutting*

From each panel, 6 DCB specimens and 6 ENF specimens were cut and the edges were polished in order to accurately locate the end of the Teflon insert (the delamination tip).

For Mode I samples (Fig. 8), opening forces were applied to the DCB specimens through loading tabs that were fixed onto the initially delaminated end. Loading tabs were bonded onto the ends of DCB specimens with a double-sided tape adhesive (Metlbond 1113), which were separately cured at 100 °C for 120 min. The tabs span the entire width of the specimen, and a steel pin linked them to a loading fixture of the testing equipment (MTS insight) fitted with a 500N load cell (Fig. 9). The initial delamination length, a_0, was measured from the center of the pinhole to the end of the Teflon insert.

Mode II (Fig. 13) specimens were subjected to three-point bending loads and were simply supported by two rollers at the bottom. The initial delamination length, a_0, was measured from the center of the supporting roller on the delaminated end to the end of the Teflon insert.

2.3. *Mode I interlaminar fracture toughness test and data analysis*

Mode I tests were performed at a loading rate of 0.5 mm/min and unloading rate of 25 mm/min. The crosshead displacement and the corresponding reaction force exerted by the

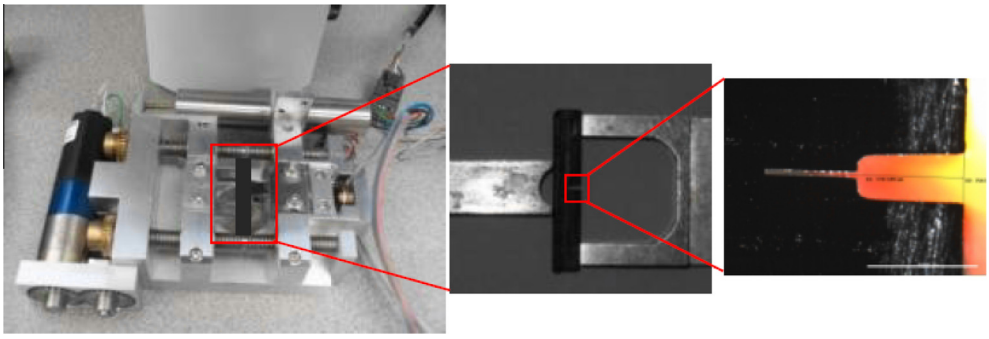

Fig. 2 – Fullam testing stage with the SENB sample mounted. (A color version of this figure can be viewed online.)

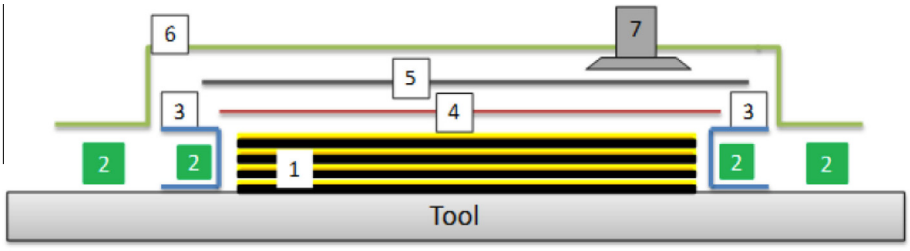

1. Carbon Fibre / Resin 2. Sealing compound 3. Fibreglass bleeder
4. Release film 5. Breather 6. Bagging film 7. Vacuum port

Fig. 4 – Vacuum bagging sequence. (A color version of this figure can be viewed online.)

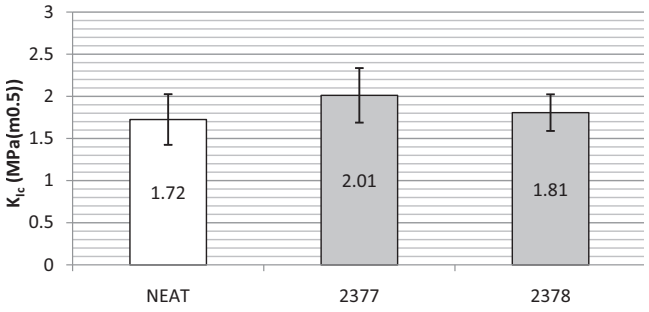

Fig. 5 – Fracture toughness of MWNT modified resin film.

specimens were captured at 2 s intervals with a data-acquisition software (MTS TestWorks 4). Load and displacement were then related to delamination length as measured with a ruler on the specimen edges.

Delamination begins when the initial portion of the load–displacement curve deviates from linearity. This critical load was used to calculate the value for initiation fracture toughness. Delamination continued to grow in an instantaneous and unstable manner, which translated into a saw-tooth relationship between load and crosshead displacement. Delamination growth occurred at the top of the saw-tooth, after which the strain energy of the material decreased instantaneously. Incremental delamination growth was on average 1–5 mm in length, and the delamination was allowed to grow for 55 mm. It was therefore possible to capture over ten distinct delamination growth increments for all specimens. Instability associated with delamination growth was minimized by selecting the lowest displacement rate in accordance with the ASTM D5528-01 standard.

The crosshead displacement (δ), load (P) and delamination length (a) were collected at each incremental crack growth point. The fracture toughness may therefore be associated with each of these points, using specimen geometry and the data reduction techniques presented in ASTM D5528-01. Three data reduction methods for calculating G_{Ic} values are used in the ASTM standard: a modified beam theory (MBT), a compliance calibration method (CC), and a modified compliance calibration method (MCC).

The average value of the G_{Ic} initiation for the MWNT modified specimens was compared to the average G_{Ic} initiation value of the neat resin specimens. The G_{Ic} propagation value for each material system was also calculated as the average of the propagation values for the 5 specimens. This G_{Ic} propagation value was then used to determine the effect of MWNT modification of composite panels.

2.4. *Mode II interlaminar fracture toughness test and data analysis*

Bending forces were applied to the Mode II End-Notched Flexure (ENF) specimens through a three-point bending setup.

Two Mode II interlaminar fracture toughness values were calculated for each sample: (1) Non-precracked (NPC) toughness (Fig. 14) and (2) Precracked (PC) toughness (Fig. 15).

The first fracture test was performed considering the end of the Teflon insert as the delamination tip (non-precracked fracture test). The initial delamination length was set to

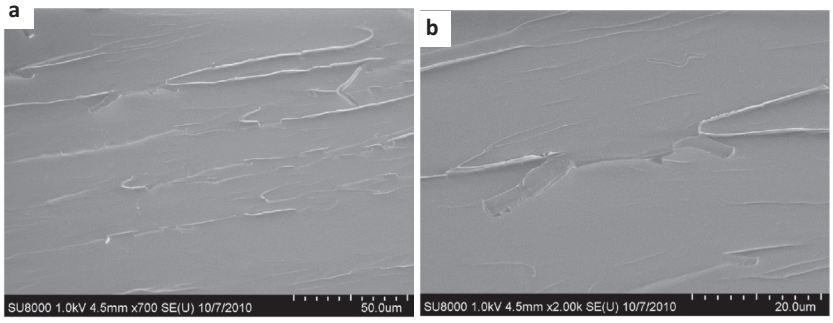

Fig. 6 – SEM images of the fractured surface of the neat polymer samples (MWNT system) at different magnifications (a - 700x, b - 2000x).

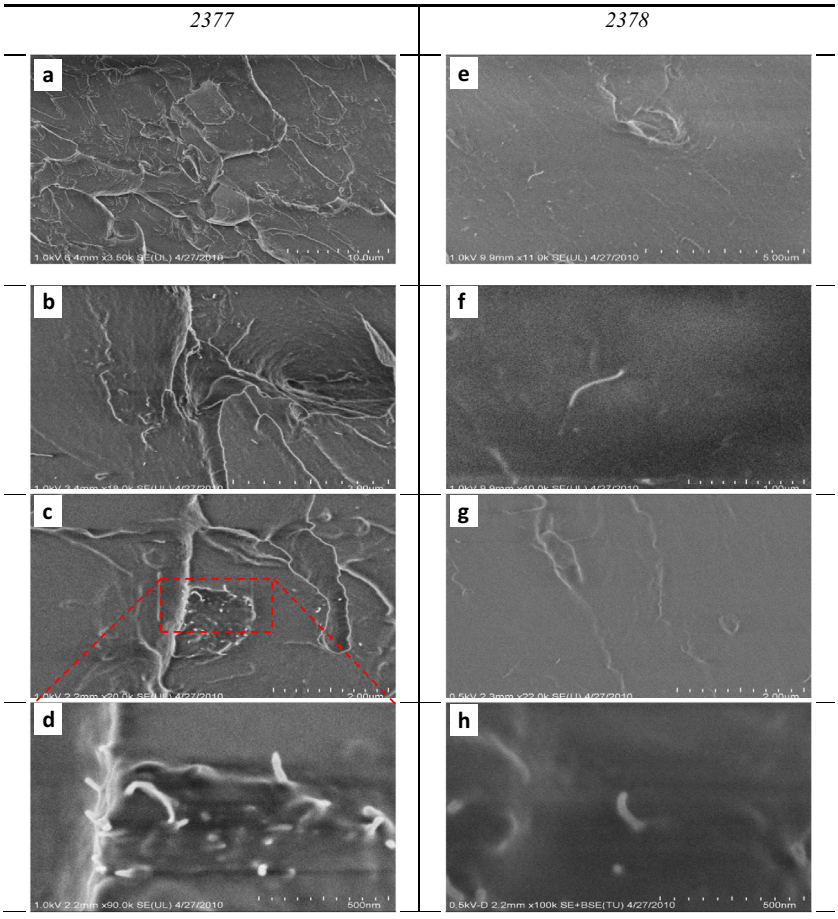

Fig. 7 – SEM images of fractured surface of 2377 samples (a–d) and 2378 samples (e–h). (A color version of this figure can be viewed online.)

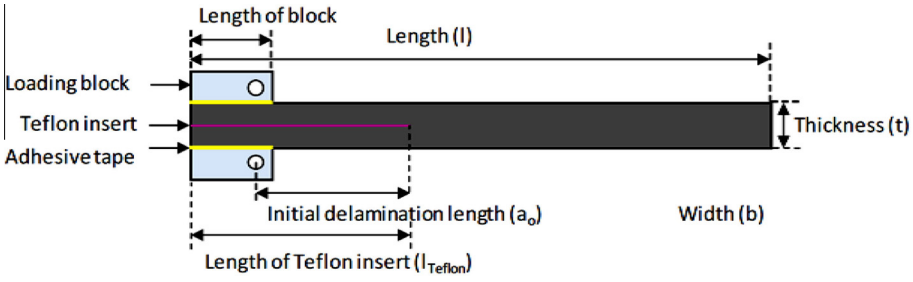

Fig. 8 – Schematic of the Mode I DCB sample with loading blocks attached. (A color version of this figure can be viewed online.)

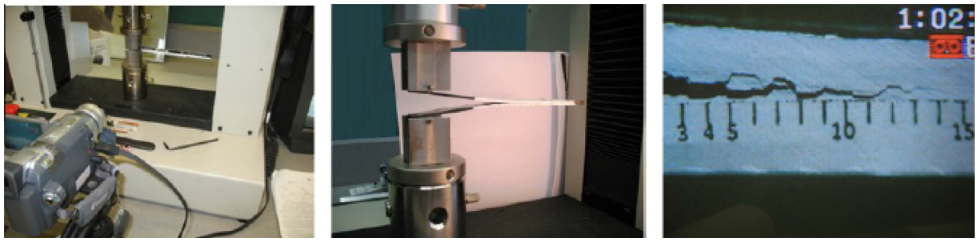

Fig. 9 – Mode I sample testing with the MTS insight machine and a video camera to capture the crack propagation. (A color version of this figure can be viewed online.)

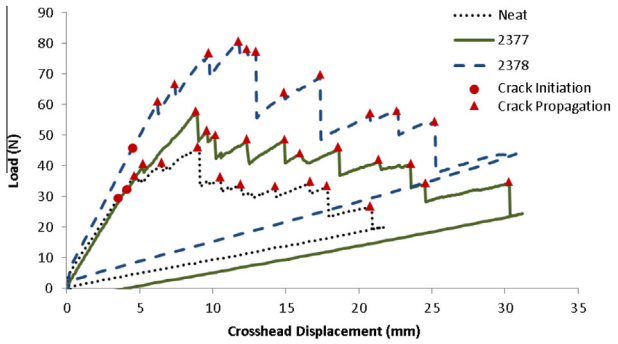

Fig. 10 – Load–displacement curves neat and MWNT modified DCB samples. (A color version of this figure can be viewed online.)

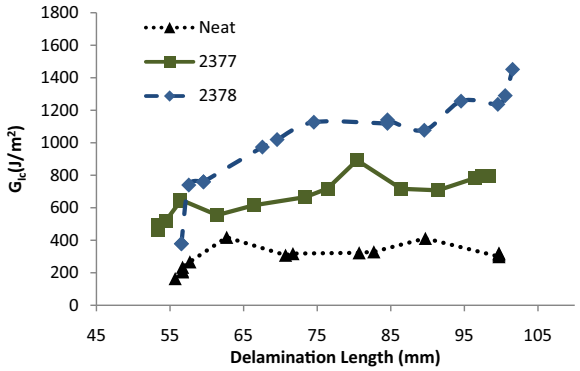

Fig. 11 – R-curve values comparing neat vs. MWNT modified DCB samples. (A color version of this figure can be viewed online.)

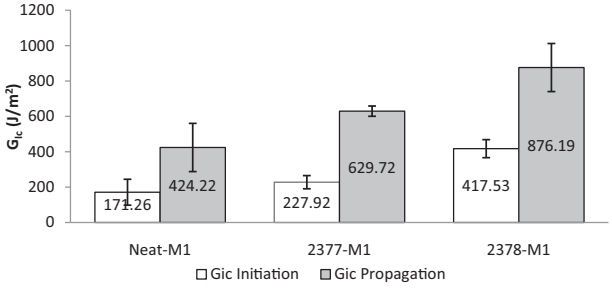

Fig. 12 – Average Mode I initiation and propagation values for neat and MWNT modified samples.

30 mm (a_0) from the crack tip. Displacement was applied to the specimen until a drop in load occurred, and the specimen was then unloaded. The point where the crack propagation stopped was taken as the new crack tip. The specimen was then repositioned such that the distance between the new tip and the center of the support roller on the delaminated end was equal to the original initial delamination length of 30 mm. The test was then restarted with this new configuration (precracked fracture test). Through data reduction, two candidate values for initiation toughness were obtained in both configurations, for a total of four values. The lowest of these four values were selected as the G_{IIc}.

The two fracture tests (non-precracked and precracked fracture tests) were both preceded by two compliance calibration (CC) tests. The objective was to quantify the compliance of each configuration which is used to find the Mode II interlaminar fracture toughness.

From the unloading data of the non-precracked fracture test, the value of a_{calc} was calculated, using:

$$a_{calc} = \left(\frac{C_u - A}{m}\right)^{1/3} \quad (1)$$

where C_u is the compliance of the non-precracked test unloading line. A and m were determined using a linear least-squares regression of the 3 NPC compliances versus the crack length, determined using:

$$C = A + ma^3 \quad (2)$$

where A is the intercept and m is the slope. The three compliances were those from the CC tests and the NPC fracture test. Once the a_{calc} was calculated, it was marked as the new pre-cracked crack tip. The specimen fracture toughness for both non-precracked and the pre-cracked tests were determined using:

$$G_Q = \frac{3mP_{Max}^2 a_0^2}{2B} \quad (3)$$

where m is the compliance calibration coefficient (Eq. (2)), P_{max} is the maximum load from the fracture test, a_0 is the crack length of the fracture test and B is the average specimen length.

3. Results and discussion

3.1. Resin characterization

3.1.1. Fracture toughness

The results of Mode I fracture toughness test is shown in Fig. 5. These tests are the results of plain strain fracture toughness test according to the ASTM D5045, under the 3-point bending. It was calculated that for the NEAT samples the fracture toughness varies as 1.72 ± 0.3 MPa $m^{1/2}$, for the 2377 samples the fracture toughness varies as 2.01 ± 0.3 MPa $m^{1/2}$ and for the 2378 samples the fracture

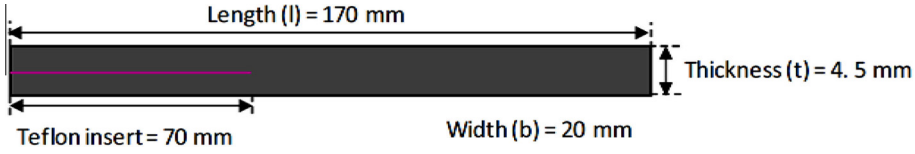

Fig. 13 – Schematic of the Mode II DCB sample. (A color version of this figure can be viewed online.)

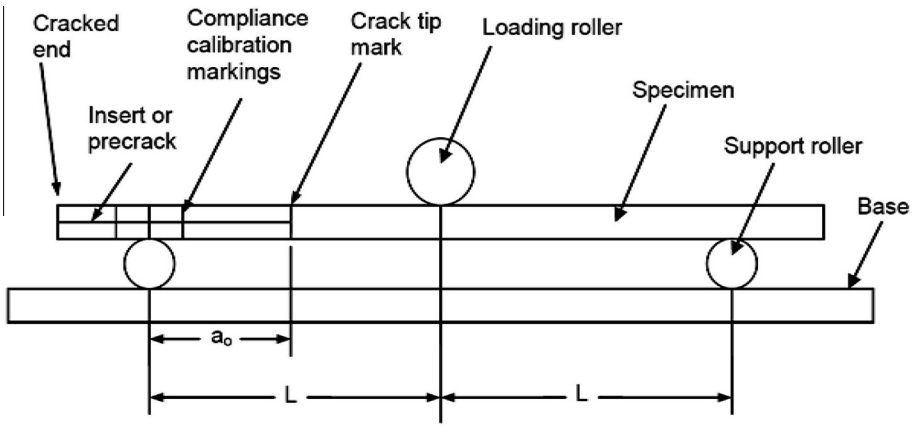

Fig. 14 – Schematic of Mode II rollers and sample marking and dimensions for the NPC test.

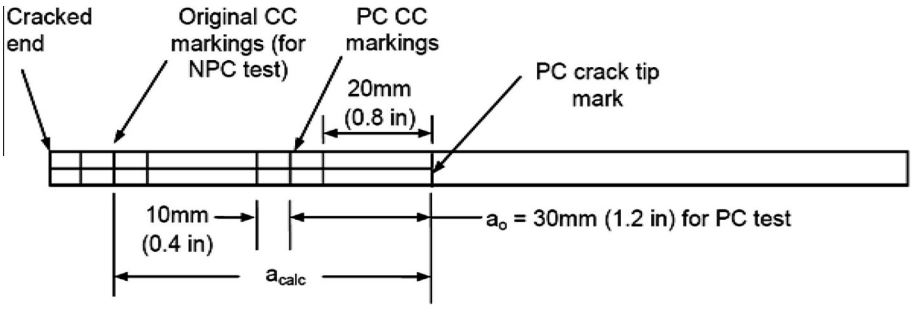

Fig. 15 – Schematic of Mode II sample with markings and dimensions of the PC test.

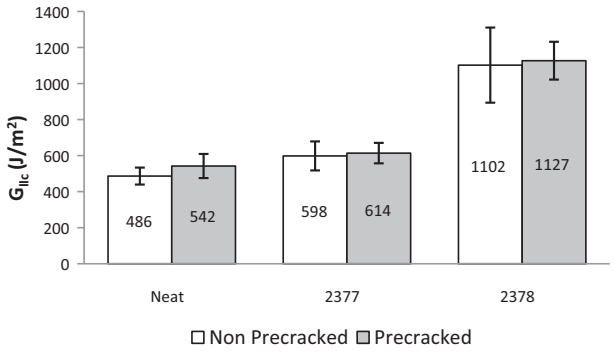

Fig. 16 – Average Mode II interlaminar fracture toughness values.

toughness varies as 1.81 ± 0.2 MPa $m^{1/2}$. When compared to the base resin, the fracture toughness of the 2377 and 2378 samples improved by 17% and 5% respectively and the 2377 demonstrated the highest fracture toughness values. In order to understand better the results, the fractured surfaces of the samples were studied under the SEM, to identify the potential toughening mechanisms.

3.1.2. *Fractography*

The SEM images of the fractured surface were taken with a Hitachi SU-8000 Cold Field Emission SEM, as a low voltage SEM was required to avoid surface charging of the non-conductive MWNT modified polymers. With this SEM, it was also possible to avoid the process of sputter coating the

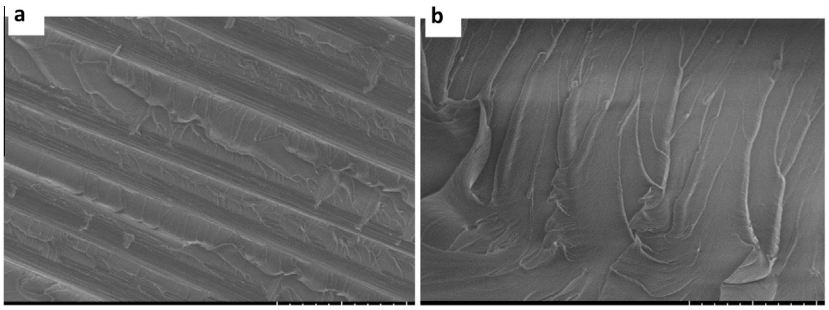

Fig. 17 – SEM analysis of the delaminated surface – Neat composite laminates (a - fibre marks, b - resin rich region near the crack).

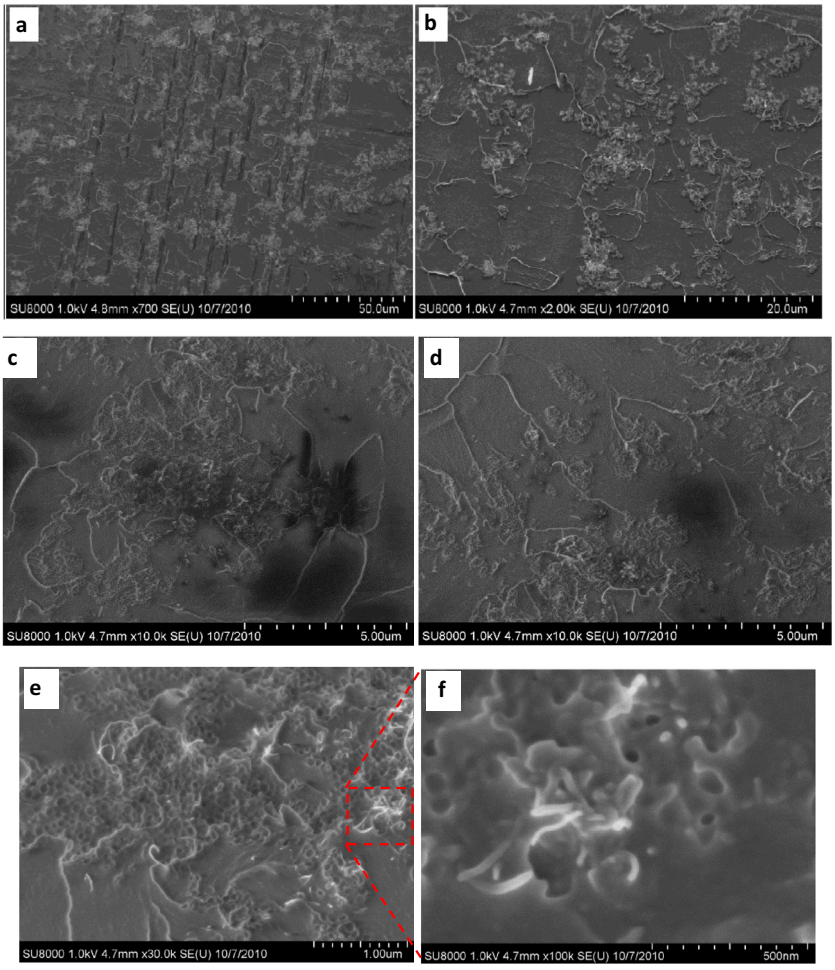

Fig. 18 – SEM analysis of the delaminated surface – 2377 MWNT composite laminates (a - 700x, b - 2000x, c and d - 10000x, e and f - MWNT pulled out). (A color version of this figure can be viewed online.)

polymer samples with a conductive metal layer, which could affect the surface morphology.

The SEM images of the fractured surface taken with the Hitachi SU-8000 Cold Field Emission SEM are shown in Fig. 6 for the neat polymer system. As seen from the images, there were river lines on the surface confirming a brittle fracture. But other than the river lines, the fracture surface was very smooth and shiny, with no specific features.

For the MWNT-modified specimens (2377 and 2378), a rough surface with several toughening features on the surface, such as crack pinning and MWNT pull out was observed. Fig. 7 compares the fracture surface of the 2377 specimens with the 2378 specimens at different magnification levels. The surface of the 2377 specimens were rougher compared to the 2378 and more MWNT pull-out was observed on the surface of the 2377 samples. These features on the SEM images explain the higher fracture toughness for the 2377 samples. Also, seen in Fig. 7(c) (the red square), in certain areas, the agglomerated MWNTs caused a local polymer failure creating a concave surface. This process introduced a new energy dissipation mechanism for fracture toughening.

3.2. *MWNT modified composite characterization*

3.2.1. *Mode I delamination properties*

Typical load–displacement curves comparing neat and MWNT-modified DCB samples are shown in Fig. 10. Both neat and MWNT-modified samples demonstrated a linear load–displacement relation up to the crack initiation point. However, the MWNT modified samples sustained a higher initiation load. The load–displacement data were used to generate the resistance curves shown in Fig. 11. The results of G_{Ic} initiation and propagation for all the specimens were then averaged and reported as the Mode I interlaminar fracture toughness, shown in Fig. 12.

For the case of MWNT resin film DCB samples, the 2377 sample showed a 33% and 48% increase in the initiation and propagation G_{Ic}, respectively, compared to the base laminate. For the 2378 samples, G_{Ic} initiation and propagation values were increased by 143% and 106%, respectively. The 2377 samples contained only MWNT whereas the 2378 contained MWNT as well as a thermoplastic toughener. The thermoplastic toughener (the chemistry of which is protected under a

provisional patent by Nanoledge Inc.) is designed to improve the fracture toughness by creating rubbery nanodomains to absorb fracture energy. These improvements clearly showed major toughening contributions through a synergistic mechanism between MWNTs role (crack bridging, pull-out, crack pinning, crack deflection) and thermoplastic toughener (rubber bridging, shear yielding). The rising R-curve (Fig. 11) was a sign of MWNT-bridging and other toughening mechanisms such as crack pinning and bowing.

An important observation from the Mode I delamination results (G_{Ic}) is in the effectiveness of MWNTs in composites compared to the fracture toughness of the MWNT-modified resin (SENB samples). The polymer toughness for the 2377 and 2378 increased by 17% and 5%, whereas for the composite DCB samples, the initiation G_{Ic} increased by 33% and 143%, respectively. This trend can be explained by looking at the source of energy dissipation as crack grows, i.e. fiber/matrix debonding [26]. In the DCB samples, the nature of the interaction among the MWNTs, the polymer and the fiber is different from the interaction between the resin and MWNTs in the SENB samples [27,28]. Also, the carbon fabric acts as a network that limits the movement of MWNTs during the cure process leading to a more uniform MWNT dispersion in DCB specimens. It should also be noted that the standard loading rates and the crack tip geometry are different between the SENB sample and DCB samples [29,30]. The crack tip geometry influences G_{Ic} results particularly for crack initiation. The SENB specimens contained a sharp, natural pre-crack whereas DCB specimens contained a Teflon insert (crack initiator) which may have a blunting effect, which could in turn result in a higher G_{Ic} for crack initiation.

The average Mode I interlaminar initiation toughness values were lower than the propagation values. The reason for the higher propagation values was that the first incremental delamination started from the end of the Teflon insert (crack initiator), whereas, when the crack propagated, toughening mechanisms such as fiber/MWNT bridging kicked in requiring higher energy to further grow the crack [31,32].

In summary, for Mode I delamination results, addition of the MWNTs improved the initiation and propagation G_{Ic}. Higher interlaminar propagation toughness values can be attributed to MWNT pull out from the matrix polymer and other MWNT toughening mechanisms such as crack deviation and crack pinning, which will be discussed in detail in the Fractography section.

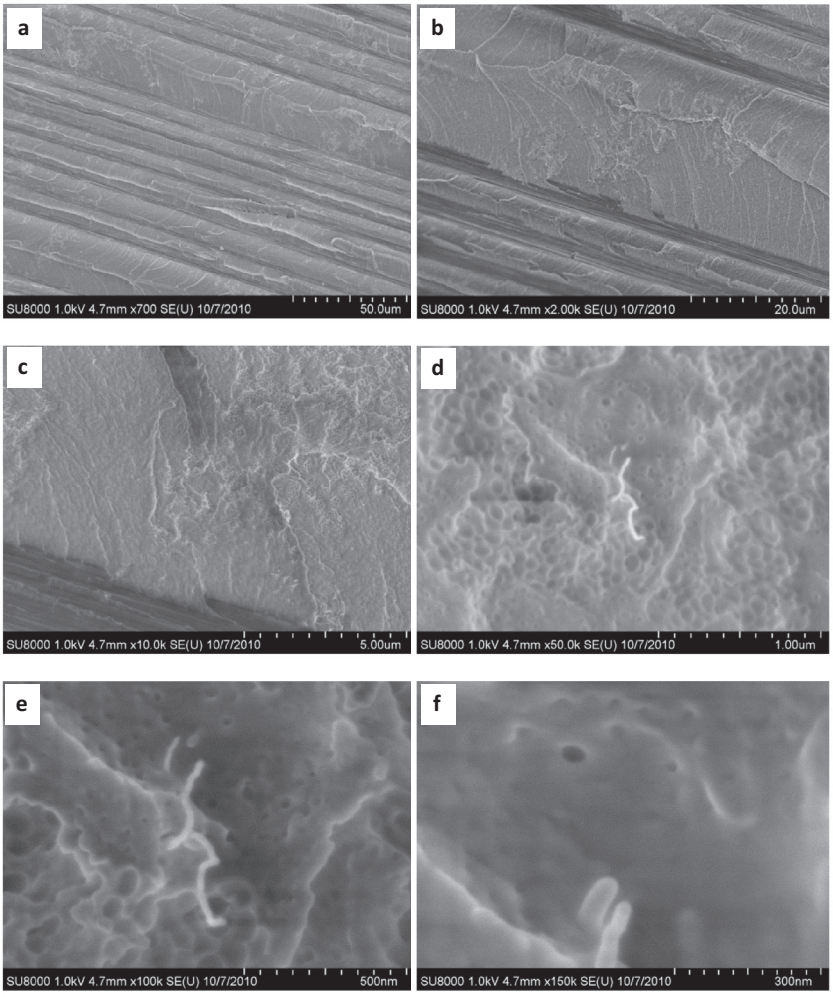

Fig. 19 – SEM analysis of the delaminated surface – 2378 MWNT composite laminates (a - 700x, b - 2000x, c rough areas between nanotubes, d, e and f - magnification of area c).

3.2.2. *Mode II delamination properties*

The objective of the non-precracked (NPC) and the precracked (PC) fracture tests was to capture delamination initiation in Mode II, since delamination growth was highly unstable [33]. The fracture toughness results of 3 specimens for each system were averaged and are shown in Fig. 16. As seen from the figure, addition of MWNTs increased the Mode II interlaminar fracture toughness. The NPC Mode II interlaminar fracture toughness values improved by 23% and 127% for the 2377 and 2378 samples, respectively. Whereas, the PC Mode II interlaminar fracture toughness values were increased by 13% and 108%, respectively. Even though the 2378 samples with MWNTs and nanofiller performed better than the 2377 samples, it should also be noted that the standard deviations from the average results was larger.

3.2.3. *Fractography*

The Hitachi SU-8000 Cold Field Emission SEM was used to further study the fracture surface of the composite laminates after delamination tests. The results of the Mode I fracture surface of the composite laminates with no MWNT at different magnifications are shown in Fig. 17. Different locations on the surface at 2000× magnification are shown in Fig. 17(a and b). Fig. 17(a) was taken at a location where the resin got detached from the fibers, and Fig. 17(b) was taken near the crack, in a resin-rich region.

For the MWNT-modified composites, the Mode I fracture surface was considerably rougher compared with the neat resin laminates. The results for the 2377 and 2378 MWNT laminate are shown in Figs. 18 and 19, respectively. For both formulations, an important observation was the interaction of the resin film with the carbon fiber fabric. As can be seen in Figs. 18(a) and 19(a), the fibers were covered with a layer of modified resin, with relatively well-dispersed MWNTs. This stronger interaction was the major difference between the neat composite laminates and the MWNT modified ones, leading to higher delamination resistance. For both MWNT-modified formulations (2377 and 2378), MWNTs were agglomerated into MWNT-rich islands. However, for the 2377 formulation, between the MWNT agglomerated islands, the fracture surface was smooth, whereas for the 2378 formulation, the surface was considerably rough. Also, for the 2377 formulation, on each MWNT-rich island, several MWNTs were pulled out as shown in Fig. 18(e and f), which clearly contribute to higher energy consumption and consequently, higher resistivity to crack growth.

For the 2378 formulation, the same toughening mechanisms existed as the 2377 formulation as seen in Fig. 19(e and f), except that, the areas between the MWNT islands were rough, due to the thermoplastic toughener that was added to improve the delamination properties, Fig. 19(c and d).

4. Conclusions

In this paper, the effect of Multi Wall Carbon Nanotubes (MWNT) on the delamination properties of composite laminates was investigated. Mode I and Mode II tests were conducted to verify the potential of MWNTs in enhancing the delamination properties of laminates. Table 1 summarizes the improvements that were observed for each test.

The MWNT-modified polymers showed a relatively minor improvement in the mechanical properties. On the other hand, the laminated composites exhibited major improvement in delamination properties as a result of adding MWNTs. The possible reasons for this behavior are as follows:

(1) The carbon fiber fabric in the composite samples acted as a network preventing the movement of MWNT bundles and consequently improved dispersion quality compared to the polymer samples.
(2) During the end-notch fracture toughness test of resins, the crack front has the freedom to propagate in any direction along the specimen width. As a result, the crack could progress along the path with lowest resistance against the crack growth. This path could potentially include ones with MWNT impurities which tend to have weak interfacial interactions with the surrounding polymer chains. However, for the case of Mode I and Mode II interlaminar fracture toughness tests, the crack growth was only limited to the 7 μm-thick interlaminar layer. As a result, MWNTs in the interlaminar region could more effectively bridge the crack front.

This contrasting behavior in the fracture toughness properties of polymers vs. composite laminates was explained by studying the fracture surface through Scanning Electron Microscopy (SEM). The SEM images gave additional information about the morphology of the fracture surface and toughening mechanisms. The toughening mechanisms included MWNT pull-out, crack pinning, crack deviation, and MWNT peel-off. By comparing the morphology of the polymer based samples with those of composite laminates, it was concluded

Table 1 – Summary of fracture toughness improvement.

Percentage increase with respect to neat resin			MWNT resin film	
			2377 (%)	2378 (%)
Polymer	Stress intensity	K_{Ic}	17	5
Composite	Mode I	G_{Ic} initiation	33	143
		G_{Ic} propagation	48	106
	Mode II	G_{IIc} NPC	23	127
		G_{IIc} PC	13	108

that there were more toughening features on the surface of delaminated composites. The morphology of the fracture surface also demonstrated a better dispersion of MWNT's as the carbon fibers seem to act as a network, preventing MWNTs to move freely and re-agglomerate.

Acknowledgements

The authors would like to acknowledge the contribution of Dr. Abdelatif Atarsia from Bombardier Aerospace on the manufacturing of composite laminate panels.

REFERENCES

[1] Hull D. An introduction to composite materials. Cambridge University Press; 1981.
[2] Koutsky J et al. Evaluation of fracture energies of composites using cantilever beam techniques. In: Organic coatings and applied polymer science proceedings, 1983.
[3] Garg A, Ishai O. Hygrothermal influence on delamination behavior of graphite/epoxy laminates. Eng Fract Mech 1985;22(3):413–27.
[4] Keary PE et al. Mode I interlaminar fracture toughness of composites using slender double cantilevered beam specimens. J Compos Mater 1985:154–77.
[5] Whitney JM, Browning CE, Hoogsteden W. A double cantilever beam test for characterizing Mode I delamination of composite materials. J Reinf Plast Compos 1982:297–313.
[6] Rhodes MD. Damage tolerance research on composite compression panel. NASA-CP 1980;2142:107–43.
[7] Garg AC, Mai Y-W. Failure mechanisms in toughened epoxy resins – a review. Compos Sci Technol 1988;31(3):179–223.
[8] Gojny FH et al. Influence of different carbon nanotubes on the mechanical properties of epoxy matrix composites – a comparative study. Compos Sci Technol 2005;65(15–16):2300–13.
[9] Thostenson ET, Chou T-W. Processing-structure-multi-functional property relationship in carbon nanotube/epoxy composites. Carbon 2006;44(14):3022–9.
[10] Blanco J et al. Limiting mechanisms of Mode I interlaminar toughening of composites reinforced with aligned carbon nanotubes. J Compos Mater 2009;43(8):825–41.
[11] Liyong Tong, Xiannian Sun, Ping Tan. Effect of long multi-walled carbon nanotubes on delamination toughness of laminated composites. J Compos Mater 2008;42(1):5–23.
[12] Tugrul Seyhan A, Tanoglu M, Schulte K. Mode I and Mode II fracture toughness of E-glass non-crimp fabric/carbon nanotube (CNT) modified polymer based composites. Eng Fract Mech 2008;75(18):5151–62.
[13] Wicks SS, de Villoria RG, Wardle BL. Interlaminar and intralaminar reinforcement of composite laminates with aligned carbon nanotubes. Compos Sci Technol 2009;70(1):20–8.
[14] Bauhofer W, Kovacs JZ. A review and analysis of electrical percolation in carbon nanotube polymer composites. Compos Sci Technol 2009;69(10):1486–98.
[15] Potschke P, Fornes TD, Paul DR. Rheological behavior of multiwalled carbon nanotube/polycarbonate composites. Polymer 2002;43(11):3247–55.
[16] Qian H et al. Carbon nanotube-based hierarchical composites: a review. J Mater Chem 2010;20(23):4751–62.
[17] Fan Z, Hsiao K-T, Advani SG. Experimental investigation of dispersion during flow of multi-walled carbon nanotube/polymer suspension in fibrous porous media. Carbon 2004;42(4):871–6.
[18] Sadeghian R et al. Manufacturing carbon nanofibers toughened polyester/glass fiber composites using vacuum assisted resin transfer molding for enhancing the mode-I delamination resistance. Compos A Appl Sci Manuf 2006;37(10):1787–95.
[19] Gojny FH et al. Influence of nano-modification on the mechanical and electrical properties of conventional fibre-reinforced composites. Compos A Appl Sci Manuf 2005;36(11):1525–35.
[20] Hubert P et al. Synthesis and characterization of carbon nanotube-reinforced epoxy: correlation between viscosity and elastic modulus. Compos Sci Technol 2009;69(14):2274–80.
[21] Kinloch IA, Roberts SA, Windle AH. A rheological study of concentrated aqueous nanotube dispersions. Polymer 2002;43(26):7483–91.
[22] Kinloch A et al. The effect of silica nano particles and rubber particles on the toughness of multiphase thermosetting epoxy polymers. J Mater Sci 2005;40(18):5083–6.
[23] Kinloch AJ et al. Toughening structural adhesives via nano- and micro-phase inclusions. J Adhes 2003;79(8):867–73.
[24] Bayer M. Baytubes development product C150 P2006.
[25] ASTM, ASTM D5528 – 01 standard test method for Mode I interlaminar fracture toughness of unidirectional fiber-reinforced polymer matrix composites, 2007.
[26] Anderson TL. Fracture mechanics: fundamentals and applications. Florida: CRC Press; 1994.
[27] Jordan WM, Bradley WL. The relationship between resin mechanical properties and Mode I delamination fracture toughness. J Mater Sci Lett 1988;7(12):1362–4.
[28] Siddiqui NA et al. Mode I interlaminar fracture behavior and mechanical properties of CFRPs with nanoclay-filled epoxy matrix. Compos A Appl Sci Manuf 2007;38(2):449–60.
[29] Compston P, Jar PYB, Takahashi K. The use of crack opening displacement rate to assess matrix-to-composite Mode I toughness transfer. J Mater Sci Lett 2000;19(1):17–9.
[30] Compston P et al. The transfer of Matrix toughness to composite Mode I interlaminar fracture toughness in glass-fibre/vinyl ester composites. Appl Compos Mater 2002;9(5):291–314.
[31] Karger-Kocsis J. Stick-slip type crack growth during instrumented high-speed impact of HDPE and HDPE/SELAR discontinuous laminar microlayer composites. J Macromol Sci Part B Phys 2001;40(3):343–53.
[32] Webb TW, Aifantis EC. Crack growth resistance curves and stick-slip fracture instabilities. Mechan Res Commun 1997;24(2):123–30.
[33] Cowley KD, Beaumont PWR. The interlaminar and intralaminar fracture toughness of carbon-fibre/polymer composites: the effect of temperature. Compos Sci Technol 1997;57(11):1433–44.